Biomedicine & Pharmacotherapy 135 (2021) 111189

Contents lists available at ScienceDirect

Biomedicine & Pharmacotherapy

journal homepage: www.elsevier.com/locate/biopha

Original article

Mycophenolate mediated remodeling of gut microbiota and improvement of gut-brain axis in spontaneously hypertensive rats

Iñaki Robles-Vera [a,1], Néstor de la Visitación [a,1], Marta Toral [b,c,1], Manuel Sánchez [a,d], Manuel Gómez-Guzmán [a,d,*], Rosario Jiménez [a,b,d], Miguel Romero [a,d,2], Juan Duarte [a,b,d,2,*]

[a] Department of Pharmacology, School of Pharmacy and Center for Biomedical Research (CIBM), University of Granada, 18071, Granada, Spain
[b] Ciber de Enfermedades Cardiovasculares (CIBERCV), Spain
[c] Gene Regulation in Cardiovascular Remodeling and Inflammation Group, Centro Nacional de Investigaciones Cardiovasculares (CNIC), Madrid, Spain
[d] Instituto de Investigación Biosanitaria de Granada, ibs.GRANADA, Granada, Spain

ARTICLE INFO

Keywords:
Mycophenolate
Gut dysbiosis
Hypertension
Oxidative stress
Inflammation
SHR

ABSTRACT

Microbiota has a role in the host blood pressure (BP) regulation. The immunosuppressive drug mofetil mycophenolate (MMF) ameliorates hypertension. The present study analyzes whether MMF improves dysbiosis in a genetic model of hypertension. Twenty weeks old male spontaneously hypertensive rats (SHR) and Wistar Kyoto rats (WKY) were randomly divided into three groups: untreated WKY, untreated SHR, and SHR treated with MMF for 5 weeks. MMF treatment restored gut bacteria from the phyla Firmicutes and Bacteroidetes, and acetate- and lactate-producing bacteria to levels similar to those found in WKY, increasing butyrate-producing bacteria. MMF increased the percentage of anaerobic bacteria in the gut. The improvement of gut dysbiosis was associated with an enhanced colonic integrity and a decreased sympathetic drive in the gut. MMF inhibited neuroinflammation in the paraventricular nuclei in the hypothalamus. MMF increased the lower regulatory T cells proportion in mesenteric lymph nodes and Th17 and Th1 infiltration in aorta, improved aortic endothelial function and reduced systolic BP. This study demonstrates for the first time that MMF reduces gut dysbiosis in SHR. This effect could be related to its capability to improve gut integrity due to reduced sympathetic drive in the gut associated to the reduced brain neuroinflammation.

1. Introduction

Systemic arterial hypertension is a complex, multifactorial and multisystem disorder influenced by genetic and environmental factors, and the most important modifiable risk factor that contributes significantly to worldwide cardiovascular morbidity and mortality. The precise cause of elevated blood pressure (BP) often cannot be determined and its identification is still challenging. Hypertension appears to have a complex association with the state of the sympathetic nervous system, endothelial dysfunction, cardiovascular remodelling and renal dysfunction. Moreover, emerging evidence indicates that immune system dysfunction is an important factor in the pathogenesis of hypertension [1]. In fact, T cell activation modulates the development of hypertension induced by both angiotensin II or deoxicorticosterone acetate (DOCA)-salt [2].

Recently, an imbalance in the gut microbiota composition relative to

Abbreviations: BP, blood pressure; CM-H2DCFDA, 5-(and-6-)chloromethyl-2′-7′-dichlorodihydrofluorescein diacetate; DAPI, 4,6-diamidino-2-phenylindole dichlorohydrate; DHE, dihydroethidium; DNA, deoxyribonucleic acid; DOCA-salt, deoxycorticosterone acetate; F/B, Firmicutes/Bacteroidetes; FoxP3, forkhead box P3; GOLD, Genomes OnLine Database; IL, interleukin; KEGG, Kyoto Encyclopedia of Genes and Genomes pathways; L-NAME, N^G-nitro-L-arginine methyl ester; LEfSe, Linear discriminant analysis effect size; LDA, Linear discriminant analysis; LPS, lipopolysaccharide; MLN, mesenteric lymph nodes; MMF, mofetil mycophenolate; MPA, mycophenolic acid; MUC, mucin; NO, nitric oxide; OTU, operational taxonomic unit; PCA, principal component analysis; PICRUSt, phylogenetic investigation of communities by reconstruction of unobserved states; PVN, paraventricular nucleus; RDP, Ribosome Database Project; RORγ, retinoid-related orphan receptor-γ; ROS, reactive oxygen species; SBP, systolic blood pressure; SCFAs, short chain fatty acids; SHR, spontaneously hypertensive rats; Th, T helper; TH, tyrosine hydroxylase; TNF-α, tumor necrosis factor-alpha; Tregs, regulatory T cells; WKY, Wistar Kyoto rats; ZO-1, zonula occludens-1.

* Corresponding authors at: Department of Pharmacology, School of Pharmacy, University of Granada, 18071, Granada, Spain.
E-mail addresses: mgguzman@ugr.es (M. Gómez-Guzmán), jmduarte@ugr.es (J. Duarte).

[1] These authors contributed equally as first authors.
[2] These authors contributed equally to the supervision of the study as senior authors.

https://doi.org/10.1016/j.biopha.2020.111189
Received 15 October 2020; Received in revised form 27 November 2020; Accepted 26 December 2020
Available online 31 December 2020

the healthy state, termed dysbiosis, has been associated with hypertension [3–6]. The characteristics of dysbiosis in spontaneous hypertensive rats (SHR) were decrease in the microbial richness, marked increase in the Firmicutes/Bacteroidetes (F/B) ratio, and decrease in acetate- and butyrate-producing bacteria and an increase in the lactate-producing bacterial population [3,5,7–9]. Bacterial derived short chain fatty acids (SCFAs) are involved in BP regulation [9,10]. Studies using fecal microbiota transplantation have demonstrated that gut flora from hypertensive animals and human increased BP, showing a cause-effect relationship [5,11], albeit the mechanisms involved in BP regulation by the microbiota have not been fully elucidated. Gut dysbiosis was associated to low intestinal integrity, which facilitates the translocation across the intestinal epithelium of bacteria and their endotoxins and metabolites, leading to CX3CR1+ cells (dendritic cells and macrophages) activation and migration to lower intestinal tract draining lymph nodes, promoting T cells activation [12].

The microbiome has a crucial part in the induction, maturation and maintenance of the host immune system. Interestingly, inhibition of T cell activation and T helper (Th)17 differentiation inhibited the hypertensive effect induced by dysbiotic microbiota from SHR, showing that immune system dysregulation induced by the gut microbiota may be, at least partially, responsible for causing hypertension [5]. However, immunosuppressive drugs, such as tacrolimus and mofetil mycophenolate (MMF) differently affect BP, whereas tacrolimus increases BP [13–15], MMF reduces it [16–21]. Tacrolimus reduces the overall number of T cells because of its inhibitory effect on calcineurin, the remaining T cells differentiate into Th17, which releases the potent proinflammatory cytokine interleukin (IL)-17, leading to endothelial dysfunction and hypertension [22]. MMF is a prodrug of mycophenolic acid (MPA), an inhibitor of inosine 5′-monophosphate dehydrogenase. This drug also depletes proliferating B and T lymphocytes due to its ability to rate-limit enzymes in de novo synthesis of guanosine nucleotides. MMF was able to prevent the development of hypertension in SHRs, Dahl salt-sensitive rats and DOCA-salt due to this pharmacological inhibition of B and T cells proliferation [16–21]. However, MMF is not a blood pressure lowering drug. Animal studies and clinical reports linking this drug to lower blood pressure occur only when immune-mediated renal disease coexists [23]. In contrast with tacrolimus, MPA *in vitro* inhibits Th17 differentiation in activated human peripheral blood mononuclear cells [24,25], and human CD4 cells, and *in vivo* in renal transplant patients [26], which could be involved in BP regulation. In fact, MMF decreased circulating and renal T cells in SHR, although MMF reduced both T cell subtypes, Th17 and T-regulatory (Tregs) [27]. Recently, tacrolimus induced-hypertension was linked to gut dysbiosis and the capacity of gut microbiota from tacrolimus-mice to induce an elevation in BP was a result of an elevation in Th17 populations and a reduction in Treg populations [28]. Similarly, it has been described that MMF influences the gut microbiome in renal transplant patients [29–32] and rodents [33]. Moreover, MMF treatment causes dynamic changes in the composition of the intestinal microbiota that may be a targetable driver of the gastrointestinal side-effects of MMF [34,35]. Furthermore, under normotensive conditions, chronic MMF treatment did not significantly change the overall gut microbial composition, and phyla, families and genera proportion [36]. However, it is unknown whether the modulation of the immune system by MMF normalizes the gut dysbiosis under hypertensive conditions. Thus, the aim of this study was to analyze the effects of MMF in the gut microbiota and T-cell populations in a genetic model of hypertension.

2. Materials and methods

2.1. Animals and experimental groups

The experiments performed in this study followed the European Union regulations and requirements on the protection of animals used for scientific purposes. All protocols were approved by the Ethics Committee of Laboratory Animals of the University of Granada (Spain; permit number 03-CEEA-OH-2013). Animal studies are reported in compliance with the ARRIVE guidelines [37]. Twenty weeks old male SHR and Wistar Kyoto (WKY) rats from Envigo (RRID:RGD5508396, Barcelona, Spain) were purchased for this study. The animals were arbitrarily allotted into three groups: a) untreated WKY (WKY, 1 mL of tap water/day, n = 8), b) untreated SHR (SHR, 1 mL of tap water/day, n = 8), and c) and SHR treated with MMF (SHR-MMF, 20 mg/Kg/day by gavage for 5 weeks, n = 8). Rats were kept in individual and ventilated cages. Food and water intake were recorded daily for all groups. During the experimental period, rats had free access to tap water and chow. Body weight was measured every week. MMF treatment was stopped 2 days before the end of the experiments, to study its long-term effects without the involvement of acute administration effects.

2.2. Blood pressure measurements

A 2-week adaptation period for vehicle administration and systolic blood pressure (SBP) measurements was established prior to the start of any experimental procedures. The evolution of SBP was recorded every week at room temperature by tail-cuff plethysmography as described previously [8,9,38].

2.3. Cardiac and renal weight indices

At the experimental end point, the animals fasted for 18 h and were anesthetized with 2.5 mL/kg equitensin (i.p.). Blood was collected from the abdominal aorta. Then, the animals were euthanised *via* exsanguination. The heart was taken out and weighed, and then divided into the left ventricle and the right ventricle plus atria. All collected samples were frozen in liquid nitrogen and subsequently preserved at -80 °C.

2.4. Plasma determinations

Ice was used to cool blood samples, which were centrifuged at 3500 rpm at 4 °C for 10 min, then the plasma is frozen at −80 °C. According to the manufacturer's instructions, the Amebocyte Lysate Chromogenic Endotoxin Quantitative Kit (Lonza, Valais, Switzerland) was used to measure the plasma lipopolysaccharide (LPS) concentration.

2.5. Vascular reactivity studies

Thoracic aortic ring-shaped segments (3 mm) were obtained and placed in organ chambers filled with Krebs solution (composition in mmol/L: $CaCl_2$ 2, glucose 11, KCl 4.75, KH_2PO_4 1.2, $MgSO_4$ 1.2, NaCl 118 and $NaHCO_3$ 25) as described in previous articles [39]. The concentration-relaxation responses to acetylcholine (10^{-9} -10^{-5} mol/L) were analyzed in aorta pre-contracted with phenylephrine (1 μmol/L). Nitroprusside concentration-relaxation responses (10^{-9}–10^{-6} mol/L) were performed in the dark in aortic rings denuded from endothelium pre-contracted with 1 μmol/L phenylephrine. In some rings, acetylcholine responses were studied after incubation with N^G -nitro-L-arginine methyl ester (L-NAME, a non-selective competitive inhibitor of nitric oxide synthase, 10^{-5} mol/L) or apocynin (non-selective inhibitor of NADPH oxidase activity, 10^{-4} mol/L) for 30 min. Relaxant responses were represented as a percentage of precontraction tension levels.

2.6. NADPH oxidase activity

As previously described [40], to determine the NADPH oxidase activity in the intact aortic ring, we utilized a lucigenin-enhanced chemiluminescence assay. The aortic rings of all experimental groups were incubated in a physiological salt solution (pH 7.4) containing HEPES with the following composition (in mmol/L) at 37 °C for 30 min: $CaCl_2$ 1.2, glucose 5.5, HEPES 20, KCl 4.6, KH_2PO_4 0.4, $MgSO_4$ 1, NaCl 119, $NaHCO_3$ 1 and Na_2HPO_4 0.15. Adding NADPH (100 μmol/L) to the

buffer containing the aortic ring, and automatically injecting lucigenin (5 μmol/L). NADPH oxidase activity was determined by measuring luminescence for 200 s periods in 5-s intervals in a scintillation counter (Lumat LB 9507, Berthold, Germany) and calculated by subtracting the basal values from those obtained in the presence of NADPH and expressed as RLU (relative light units)/min per mg of tissue for aortic rings.

As mentioned earlier [41], the NADPH oxidase activity in the paraventricular nucleus (PVN) homogenate was measured by the dihydroethidium (DHE) fluorescence assay in a microplate reader. A solution of fresh homogenate (10 μg protein) with DHE (10 μmol/L) and deoxyribonucleic acid (DNA, 1.25 μg/mL) in PBS (100 mmol/L), pH 7.4, containing 100 μmol/L DTPA and NADPH (50 μmol/L) to a final volume of 120 μL, was incubated for 30 min at 37 °C in the dark. The total fluorescence was tracked in a fluorescence spectrophotometer (Fluorostart, BMG Labtechnologies, Offenburg, Germany) using a rhodamine filter (excitation 490 nm, emission 590 nm) in a microplate reader.

2.7. Measurement of ex vivo vascular reactive oxygen species (ROS) levels and of intracellular ROS concentrations in the brain

DHE, an oxidative fluorescent dye, was used to localize and quantify ROS in aortic segments *in situ*, as previously described [40]. To summarize, aorta segments were included in optimum cutting temperature compound medium (Tissue-Tek; Sakura Finetechnical, Tokyo, Japan), snap frozen, and cut into 10 μm thick sections in a cryostat (Microm International Model HM500 OM). Sections where then placed on slides. These slides were incubated at room temperature for 30 min with DHE (10 μmol/L) in the dark, counterstaining with the nuclear stain 4,6-diamidino-2-phenylindole dichlorohydrate (DAPI, 300 nmol/L) and examined on a fluorescence microscope (Leica DM IRB, Wetzlar, Germany) in the following 24 h period. Images of the segments were then aquired and ethidium and DAPI fluorescences were quantified with the program ImageJ (version 1.32j, NIH, http://rsb.info.nih/ij/). ROS production levels were expressed as the ratio of ethidium/DAPI fluorescence.

ROS levels were measured in brain PVN homogenates *via* the fluorescent probe 5-(and-6-)chloromethyl-2′-7′-dichlorodihydrofluorescein diacetate (CM-H2DCFDA). The homogenates were prepared in lysis buffer composed of 50 mmol/L Tris−HCl (pH 7.4) containing 10 μg/mL aprotinin, 0.1 mmol/L EDTA, 0.1 mmol/L EGTA, 10 μg/mL leupeptin and 1 mmol/L PMSF. The samples (10 μg of protein) were incubated in 96-well plates with 5 μmol/L CM-H2DCFDA for 30 min at 37 °C, in the absence or presence of apocynin, a NADPH oxidase inhibitor (50 μmol/L). The intensity of the fluorescent signal was measured using a spectrofluorimeter (Fluorostart, BMG Labtechnologies, Offenburg, Germany) [41].

2.8. Lymphocyte conditioned media

Mesenteric lymph nodes (MLN) were excised from the animals and meticulously mashed with slides dipped in sterile PBS in order to reduce friction. The suspensions obtained were then filtered with 70 μm cell strainers. Following a previously detailed protocol [42], 5 μg/mL Concanavalin A was used in RPMI 1640 with 10 % fetal bovine serum and 2 mmol/L glutamine to stimulate total lymphocytes from lymph nodes (2.5×10^6/mL), and 48 mL of 10 mmol/L 6-HEPES, 100 U/mL penicillin, 100 g/mL streptomycin and 50 μmol/L β-mercaptoethanol in a 25 mL flask for 48 h. After centrifugation, the lymphocyte conditioned media were stored at -80 °C until use. IL-10 and IL-17a levels and other cytokines were measured *via* ELISA.

2.9. Flow cytometry

MLN were obtained from all animals and mashed with slides dipped in sterile PBS to decrease friction. The resulting solutions were filtered through 70μM cell strainers. 1×10^6 cells were counted for each panel. Cells were stimulated with 50 ng/mL PMA plus 1 μg/mL ionomycin for 30 min, and then incubated with a protein transport inhibitor (BD GolgiPlugTM) to enhance detection and staining of intracellular cytokines for 4 h at 37 °C. Then, cells were transferred to polystyrene tubes. The cells were blocked with anti-CD32 (clone D34-485) to avoid non-specific binding to Fc-gamma receptors, concomitantly, samples were stained with a viability dye (LIVE/DIED® Fixable Aqua Dead cell Sain Kit, Molecular Probes, Oregon, USA) for 20 min at 4 °C in the dark. Then, cells were incubated for 30 min at 4 °C for surface staining with mAbs anti-CD4 (PerCP-Vio700, clone REA482, Miltenyi Biotec, Bergisch Gladbach, Germany), anti-CD45 (APC, clone RA3-6B2 BD PharmigenTM, New Jersey, USA. The lymphocytes were then fixed and permeabilized simultaneously with the Fix/Perm Fixation/Permeabilization kit (eBioscience, San Diego, USA) and intracellular staining was achieved with mAbs anti-forkhead box P3 (FoxP3) (PE, clone FJK-16 s, eBioscience, San Diego, USA), anti-IL-17A (PE-Cy7, clone eBio17B7, eBioscience, San Diego, USA) for 30 min at 4 °C in the dark. Samples were analyzed using a CANTO II flow cytometer (BD Biosciences) and the data were analyzed with FlowJo software (Tree Star, Ashland, OR, USA) [43].

2.10. Gene expression analysis

The analysis of gene expression in aorta, colon, brain PVN, or MNL was performed by RT-PCR, as previously described [40]. Thus, total RNA from all samples was obtained by homogenization using TRI Reagent® following the manufacturer's protocol. RNA levels were quantified with the Thermo Scientific NanoDropTM 2000 Spectrophotometer (Thermo Fisher Scientific, Inc., Waltham, MA, USA) and 2 μg of RNA from all samples were reverse transcribed into cDNA using oligo(dT) primers (Promega, Southampton, UK). Polymerase chain reaction was carried out with a Techne Techgene thermocycler (Techne, Cambridge, UK). The sequences of the sense and antisense primers utilized for amplification are described in Table 1. A dilution series of standard vascular samples determined the efficiency of the reaction. To normalize mRNA expression, the housekeeping gene β-actin was utilized. The mRNA relative quantification was calculated through the ΔΔCt method.

2.11. DNA extraction, 16S rRNA gene amplification, bioinformatics

In order to analyze the bacterial populations in the gut, fresh stools were collected from six animals in each group at the experimental end point. DNA extraction from faeces was performed with G-spin columns (INTRON Biotechnology) starting from 30 mg of samples resuspended in PBS. RNAses and proteinase K were used to treated all samples. DNA concentration was determined in the samples using Quant-IT PicoGreen reagent (Thermo Fischer) and DNA samples (about 3 ng) were used to amplify the V3-V4 region of 16S rRNA gene [8]. PCR products (approx. 450 pb) included extension tails, which allowed sample barcoding and the addition of specific Illumina sequences in a second low-cycle number PCR. Individual amplicon libraries were analyzed using a Bioanalyzer 2100 (Agilent) and a pool of samples was made in equimolar concentrations. The pool was further purified and quantified. The exact concentration estimated by real time PCR (Kapa Biosystems). Finally, the resulting DNA was sequenced on an Illumina MiSeq instrument with 2×300 paired-end read sequencing at the Unidad de Genómica (Parque Científico de Madrid, Spain).

BIPES pipeline was utilized to process the raw sequences. First, if containing ambiguous bases or mismatches in the primer regions, the barcode primers were trimmed and filtered following BIPES protocol. Second, we expunged any sequences with more than one mismatch in the 40–70 bp region at each end. Third, we used 30 Ns to concentrate the two single-ended sequences for the downstream sequence analysis. Third, we carried out an UCHIME analysis (implemented in USEARCH, version 6.1) to screen out and remove chimeras in the de novo mode

Table 1
Primers for real-time RT-PCR.

mRNA targets	Descriptions (Gene ID)	Forward	Reverse
TNF-α	tumor necrosis factor-alpha (24835)	ACGATGCTCAGAAACACACG	CAGTCTGGGAAGCTCTGAGG
IL-6	interleukin-6 (24498)	GATGGATGCTTCCAAACTGG	AGGAGAGCATTGGAAGTTGG
IL-10	interleukin-10 (25325)	GAATTCCCTGGGAGAGAAGC	GCTCCACTGCCTTGCTTTTA
IL-17a	interleukin-17a (301289)	CTTCACCTTGGACTCTGAGC	TGGCGGACAATAGAGGAAAC
IL1B	Interleukin-1β (24494)	GTCACTCATTGTGGCTGTGG	GCAGTGCAGCTGTCTAATGG
CCL2	C-C Motif Chemokine Ligand 2 (24770)	CCTCCACCACTATGCAGGTC	CAGCCGACTCATTGGGATCA
IFNϒ	interferon gamma (29197)	GCCCTCTCTGGCTGTTACTG	CCAAGAGGAGGCTCTTTCCT
T-bet	T-bet (303496)	CCACCAGCACCAGACAGAGA	AACATCCTGTAATGGCTCGTG
CD3	Cluster of differentiation 3 (25710)	CGTCCGCCATCTTGGTAGAGAGAGCAT	CTACTGCTGTCAGGTCCACCTCCAC
CD11b	Cluster of differentiation 11b (25021)	GAGAACTGGTTCTGGCTTGC	TCAGTTCGAGCCTTCTT
FOXP3	forkhead box P3 (317382)	AGGCACTTCTCCAGGACAGA	CTGGACACCCATTCCAGACT
RORϒ	ROR-gamma 1(9885)	GCCTACAATGCCAACAACCACACA	TGATGAGAACCAAGGCCGTGTAGA
Occludin	Occludin (83497)	AGCCTGGGCAGTCGGGTTGA	ACACAGACCCCAGAGCGGCA
Muc2	mucin-2 (24572)	CGATCACCACCATTGCCACTG	ACCACCATTACCACCACCTCAG
MUC3	mucin-3 (687030)	CACAAAGGCAAGAGTCCAGA	AGTGTCCTTGGTGCTGCTGAATG
ZO-1	zonula occludens-1 (292994)	GCCAGCCAGTTCCGCCTCTG	AGGGTCCCGGGTTGGTG
Th	tyrosine hydroxylase (25085)	GATTGCTACCTGGAAGGAGGT	AGTCCAATGTCCTGGGAGAAC
RNP1-2	alpha defensin RNP1-2 (613220)	GGACGCTCACTCTGCTTACC	TGGATTCTTCTTGGTCGGAG
RNP3	alpha defensin RNP3 (498659)	AAGAGCGCTGTGTCTCTTGC	CAACAGAGTCGGTAGATGCG
RNP4	alpha defensin RNP4 (286958)	TCTGCTCATCACCCTTCTCC	AACAGAGACGGTAGATGCGG
RNP5	alpha defensin RNP5 (28699)	ACCAGGCTTCAGTCATGAGG	CATCCCATTGGTTCTTGGTC
GAPDH	glyceraldehyde-3-phosphate dehydrogenase (28383)	GTCGGTGTGAACGGATTT	ATGGGTTTCCCGTTGATG

(using-minchunk 20-xn 7-noskipgaps 2). In each sample, between 90,000 and 220,000 sequences were identified. All subsequent analyses were performed with 16S Metagenomics (Version: 1.0.1.0) from Illumina. The sequences were then clustered into their operational taxonomic units (OTU) using USEARCH with default parameters (USERACH61). The threshold distance was set to 0.03. Hence, when the similarity between two 16S rRNA sequences was 97 %, the sequences were classified as the same OTU. QIIME-based alignments of representative sequences were performed using PyNAST, and the Greengenes 13_8 database was used as the template file. The Ribosome Database Project (RDP) algorithm was applied to classify the representative sequences into specific taxa using the default database. The Taxonomy Database (National Center for Biotechnology Information) was used for classification and nomenclature. Bacteria were classified based on SCFA end-product, as previously described [8]. Succinctly, genera were classified into more than one group correspondingly if they were defined as producers of multiple metabolites. Bacteria were classified according to their oxygen requirements with the Genomes OnLine Database (GOLD) [8]. The metagenomic prediction was performed by phylogenetic investigation of communities by reconstruction of unobserved states (PICRUSt). Predicted metagenomes were subsequently subjected to collapse predictions into Kyoto Encyclopedia of Genes and Genomes pathways (KEGG). The obtained data were presented as relative abundance of predicted functions within the samples. The abundance of KEGG modules was calculated by summing the abundance of genes annotated to the same feature. The interest pathways were presented as relative abundance of predicted functions within the samples. The rest of the obtained data was used to analyze the variation among the groups represented by z-score analyses.

2.12. Reagents

All reagents were purchased from Merk (Barcelona, Spain) unless otherwise specified.

2.13. Statistical analysis

The Shannon, Chao, Pielou and whole observed species were calculated using QIIME (PAST 3x). Reads in each OTU were normalized to total reads in each sample. Only taxa with a percentage of reads > 0.001 % were used for the analysis. Linear Discriminant Analyze (LDA) scores greater than 2 were displayed. Taxonomy was summarized at the genus level within QIIME-1.9.0 and uploaded to the Galaxy platform [44] to generate Linear discriminant analysis effect size (LEfSe)/cladogram enrichment plots where significant enrichment was considered at a $P < 0.05$, LDA score > 2. Results are expressed as means ± SEM of measurements. The evolution of tail SBP with time was compared using the nested design, with treatment and days as fixed factors and the rat as a random factor. When the overall difference was significant comparisons were made using Bonferroni's method with an appropriate error. Analysis of the nested design was also carried out with groups and concentrations to compare the concentration-response curves to acetylcholine. The significance of functional KEEG modules was tested by Wilcoxon rank sum test. The rest of the variables were compared with two-way factor designs, where group and treatment were fixed effect factors with unequal sample sizes in the different groups. When interaction was significant Bonferroni's method was used for pairwise comparisons. $P < 0.05$ was considered statistically significant.

3. Results

3.1. Mycophenolate (MMF) treatment reduces gut dysbiosis in SHR

The composition and diversity of bacterial communities was analyzed by calculating four key ecological parameters: Chao richness, Pielou evenness, Simpsons diversity and the number of observed species. In SHR low richness and diversity with no observable changes in evenness or the number of species were found compared to those found in WKY. MMF was unable to restore these parameters (Fig. 1). When the axonometric three-dimensional principal component analysis (PCA) at genus level of the bacterial community was represented, the compositions of the faecal microbial communities of WKY and SHRs were found to be significatively different from the previously reported compositions [3,8]. In the PCA, the 2 clusters representing the fecal microbial compositions of WKY and SHR were neatly separated, indicating 2 extremely distinct gut microbial compositions. The cluster SHR-MMF shows proximity to WKY compared to SHR (Fig. 2A). The Kaiser-Meyer-Olkin test was 0.82, indicating a highly suitable sampling for PCA. The Barlett's test of sphericity was <0.05. The key bacterial population that was responsible for discriminating among groups was the the genus *Oscillospira* (loading 0.83). The percentage of bacteria from the phylum Firmicutes was significantly higher in SHR than in WKY, while the proportions of Actinobacteria and Bacteroidetes were decreased in SHR when comparing to other groups. MMF restored bacteria from the phyla

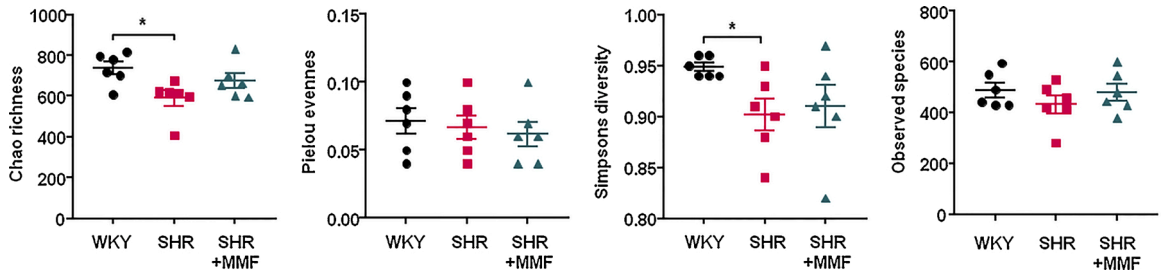

Fig. 1. Effects of Mycophenolate mofetil (MMF) in ecological parameters of the gut microbiota from spontaneously hypertensive rat (SHR). The microbial DNA from fecal samples was analyzed by 16S rRNA gene sequencing. In order to assess general differences of fecal microbial composition amongst all experimental groups, richness, evenness, diversity, and observed species were examined. Values are represented as means ± SEM. n = 6 rats per experimental group. *P < 0.05 significant differences compared with WKY.

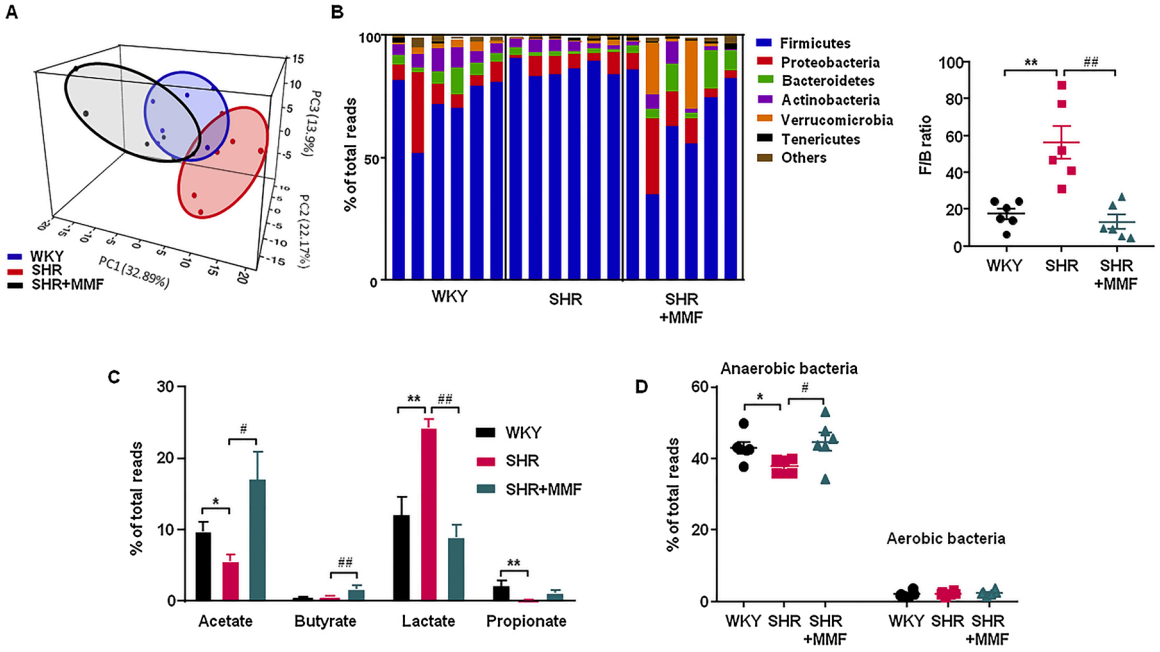

Fig. 2. Mycophenolate mofetil (MMF) induces different behaviours from the gut microbiota of spontaneously hypertensive rats (SHR). The microbial DNA from faecal samples was analyzed by 16S rRNA gene sequencing. **A**) Principal coordinate analysis in the gut microbiota from all experimental groups. **B)** Phylum breakdown of the six most abundant bacterial communities in the faecal samples was obtained from all experimental groups and Firmicutes/Bacteroidetes ratio (F/B ratio) was calculated as a biomarker of gut dysbiosis. **C)** Relative proportion of lactate-, butyrate-, acetate- and propionate-producing bacteria expressed as relative proportions of total Bacteria. **D)** Relative proportion of anaerobic and aerobic bacteria in the gut microbiota in Wistar Kyoto rats (WKY), untreated SHR and SHR treated with MMF (SHR-MMF). n = 6. Values are represented as means ± SEM. *P < 0.05 and **P < 0.01 significant differences compared with WKY. $^{\#}$P < 0.05 and $^{\#\#}$P < 0.01 significant differences compared with untreated SHR.

Firmicutes and Bacteroidetes to proportions similar to those from WKY (Table 2, Fig. 2B). The F/B ratio has been described as an indicator of intestinal dysbiosis [3] and in SHR was found ~3-fold elevated, being reduced by MMF treatment (Fig. 2B). Analyzing bacterial populations of interest, we found a significant reduction in the proportions of acetate- and propionate-producing bacteria, and higher levels of lactate-producing bacteria, with no significant differences present in the populations of butyrate-producing bacteria, in SHR compared to WKY. MMF restored the level of acetate- and lactate- producing bacteria and also, it was able to elevate the butyrate-producing bacteria (Fig. 2C). Furthermore, the populations of strict anaerobic bacteria were significantly depleted in SHR compared with WKY group, but no significant differences in strict aerobic bacteria were observed (Fig. 2D). MMF was able to restore the shift in anaerobic bacteria populations.

In Fig. 3A is displayed the alteration in bacterial taxa (class, order, family, and genus) observed in SHR through LEfSe. Relevant shifts in bacterial taxa were detected, where the relative abundance of 51 taxa were increased (green) and 19 taxa were decreased (red) in WKY compared to SHR. MMF-treated SHR also triggered substantial changes in the microbiota taxa compared to SHR group, where the relative abundance of 68 taxa were increased (green) and 12 taxa was decreased

Table 2
Effects of mofetil mycophenolate (MMF) in spontaneously hypertensive rats (SHR) on phyla changes in the gut microbiota (% of total reads).

Phylum	WKY (n = 6)	SHR (n = 6)	SHR + MMF (n = 6)
Firmicutes	72.6 ± 5.0	86.3 ± 1.4*	66.1 ± 8.5#
Proteobacteria	11.0 ± 4.8	5.8 ± 1.4	11.4 ± 4.7
Bacteroidetes	5.1 ± 1.4	1.7 ± 0.3*	7.5 ± 2.4#
Actinobacteria	6.1 ± 1.0	3.5 ± 0.6*	3.4 ± 1.5
Verrucomicrobia	1.9 ± 0.6	0.8 ± 0.3	8.6 ± 5.5
Tenericutes	0.5 ± 0.1	0.5 ± 0.1	0.8 ± 0.3
Others	1.7 ± 0.6	0.9 ± 0.1	1.4 ± 0.4

Values are expressed as mean ± SEM.
* P < 0.05 compared with the Wistar Kyoto (WKY) group.
# P < 0.05 compared with the SHR group.

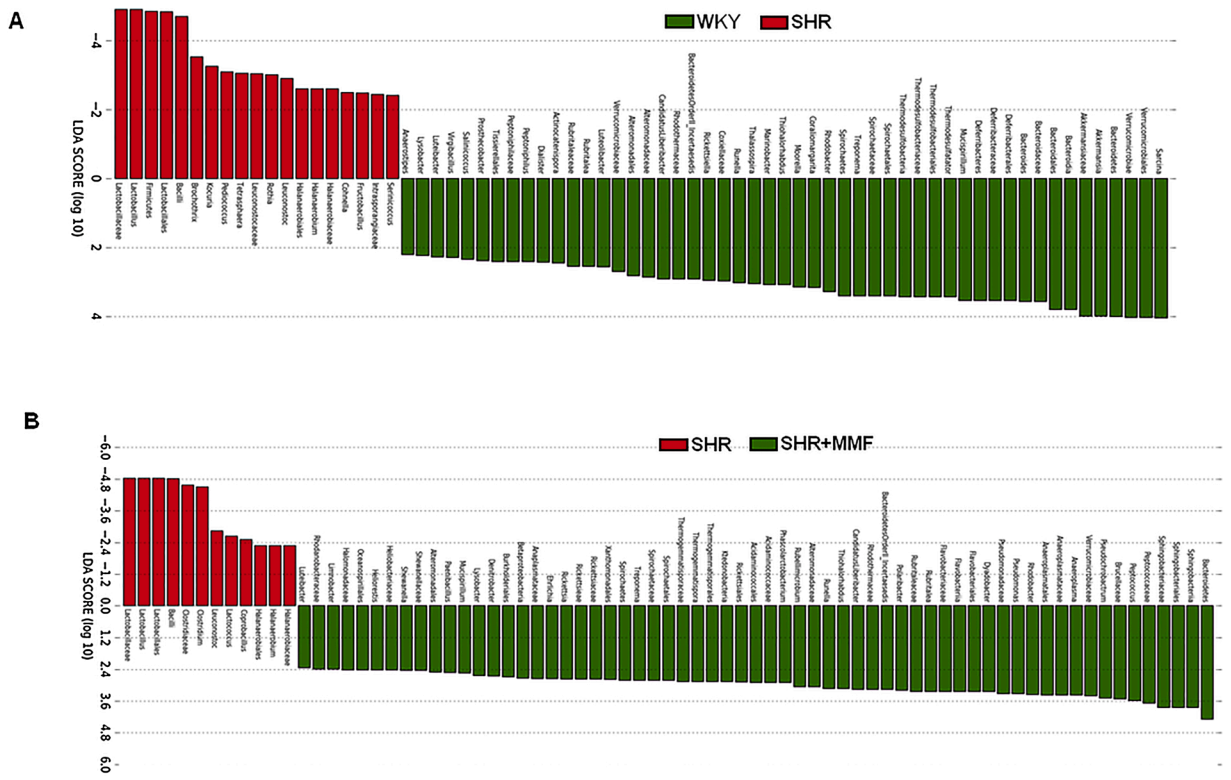

Fig. 3. Distinct shifts in the gut microbiota between Wistar Kyoto rats (WKY) and spontaneously hypertensive rats (SHR) and the Mycophenolate mofetil (MMF) treatment. A) Comparisons of microbiome changes in WKY *versus* SHR. (green bars represent WKY-enriched taxa, red bars represent SHR-enriched taxa). B) Comparisons of microbiome changes in SHR *versus* SHR-MMF (green bars represent SHR-MMF -enriched taxa, red bars represent SHR-enriched taxa). Linear discriminant analysis effect size (LEfSe) identified significantly different bacterial taxa enriched in each cohort at LDA Score > 2, $P < 0.05$. n = 6 rats per experimental group in each comparison (For interpretation of the references to colour in this figure legend, the reader is referred to the web version of this article).

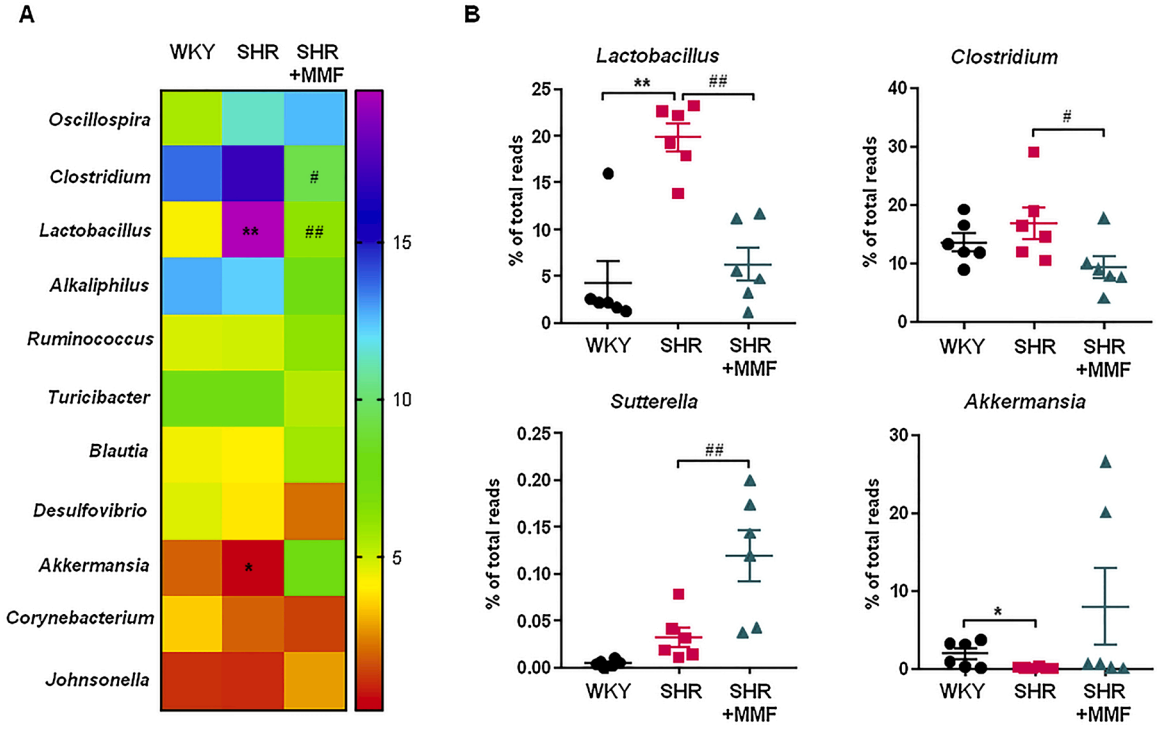

Fig. 4. Mycophenolate mofetil (MMF) induces genera shifts in the gut microbiota composition in spontaneously hypertensive rats (SHR). A) The heatmap colors represent the relative percentage of microbial genus assigned within each sample in SHR experiment. B) The relative abundance of *Lactobacillus* and *Sutterella* genus in SHR. Values are expressed as mean ± SEM (n = 6). *$P < 0.05$ and **$P < 0.01$ compared with WKY rats. $^{\#}P < 0.05$ and $^{\#\#}P < 0.01$ significant differences compared to untreated SHR group.

(red) (Fig. 3B). In the heat map was analyzed the relative expression of the eleven major genera found in SHR (Fig. 4A, B). Several authors have described the ability of certain bacteria to modulate the immune system, such as *Lactobacillus*, *Bifidobacterium*, *Sutterella* [45–47], among others. We found higher amounts of the genus *Lactobacillus* (from the *Lactobacillaceae* family) in SHR, being MMF treatment able to normalize them (Fig. 4B). In addition, no changes were found in the genus *Sutterella*, which at low levels within the gut microbiome is associated with gut immune homeostasis [47], when it was compared to the WKY group (Fig. 4B), but the MMF treatment was able to elevate it. Similarly, MMF reduced *Clostridium* content in SHR, being without significant effect in *Akkermansia* proportion, which was reduced in SHR compared to WKY (Fig. 4B).

3.2. Mycophenolate (MMF) induces an alteration in the functional profile of bacterial pathways in the intestinal microbiota of SHR

The functional alterations in the gut microbiota were evaluated across experimental groups and expressed as Z-score using KEGG database (Fig. 5). A great number of changes were found when the hypertensive group was compared to their control group. Nineteen KEGG modules were differentially modulated between WKY *vs* SHR (adjusted P value <0.05, Wilcoxon rank sum test). The MMF treatment induced a broad number of alterations in the functional pathways, in particular, in SHR-MMF forty-five pathways were found modulate when compared to SHR. Especially, pathways related to fatty acid metabolism were found changed in the SHR group (Fig. 5A). Moreover, significant differences were observed among groups in KEGG modules, when PCA was performed. A clear separation cluster was found between WKY *vs* SHR (Fig. 5B). Analyzing the role of MMF treatment on the functional alterations we found a clear separation among SHR-MMF *vs* WKY and *vs* SHR, showing a different functional bacterial profile induced by MMF.

3.3. Mycophenolate (MMF) improves intestinal integrity, endotoxemia, α-defensins production, and changed MLNs T cells in SHR

Hypertension is associated with a decrease in gut tight junction proteins expression levels, a raise in permeability and gut pathology [48]. We observed lower mRNA levels of barrier-forming junction proteins zonula occludens-1 (ZO-1) and occludin in colonic samples from SHR compared to WKY (Fig. 6A). MMF successfully restored occludin and ZO-1 expression levels in colon, pointing to an improvement in the barrier function. Additionally, high gut permeability in adult hypertensive SHR is correlated with low numbers of goblet cells [49]. Goblet cells excrete mucins, protecting the gut from pathogen invasion, and thus, regulating the gut immune response [50]. We have also found a downregulation of mucin (MUC)-2 transcripts in hypertensive groups, which was unaffected by MMF. No changes in MUC-3 in SHR compared to WKY were observed, but treatment with MMF increased its gene expression (Fig. 6A), pointing to a lower gut permeability. We quantified plasma endotoxin levels, and found them significantly increased in SHR comparing with WKY group (Fig. 6B). Remarkably, the long-term treatment with MMF decreased endotoxemia in SHR (Fig. 6B). Our results suggest an increase in intestinal permeability in SHR that would allow bacterial components (*e.g.*, LPS) to enter the blood stream. Moreover, the high mRNA concentrations of the colonic pro-inflammatory cytokines tumor necrosis factor-α (TNF-α) and IL-6 (Fig. 6C) in SHR were normalized by MMF administration.

Santisteban et al., [49] showed that the increase in the sympathetic nerve activity to the gut leads to alteration of gut junction proteins in SHR. We found an increase in the expression of tyrosine hydroxylase (TH), a crucial enzyme for the generation of noradrenaline, in the gut from SHR compared to WKY group, which was abolished by chronic MMF treatment (Fig. 6D). These results suggest that a reduction in the sympathetic tone in the gut could be associated with the possitive effects of MMF in the gut.

Epithelial intestinal cells are able to produce α-defensins, cysteine-rich cationic peptides with antibiotic activity against a broad range of microorganisms [51], to keep a stable composition of intestinal microbiota [52]. Our experiment in SHR shows a reduction in the α-defensin RNP1-2 expression levels, and increased mRNA levels of RNP3 and RNP4, without significant change of RNP5 in colon in comparison with the WKY group. MMF restored the expression levels of defensins to levels similar to those found in control groups in both experiments (Fig. 7).

As already explained, bacteria can translocate through the intestinal barrier leading to the activation of machrophages and dendritic cells and their migration to draining lymph nodes of the lower intestinal tract when under altered gut mucosal integrity [12]. These CX3CR1+ cells can also present soluble antigens to naïve CD4 + T cells, causing T cell activation. In our experiments, the number of total lymphocytes in MLNs

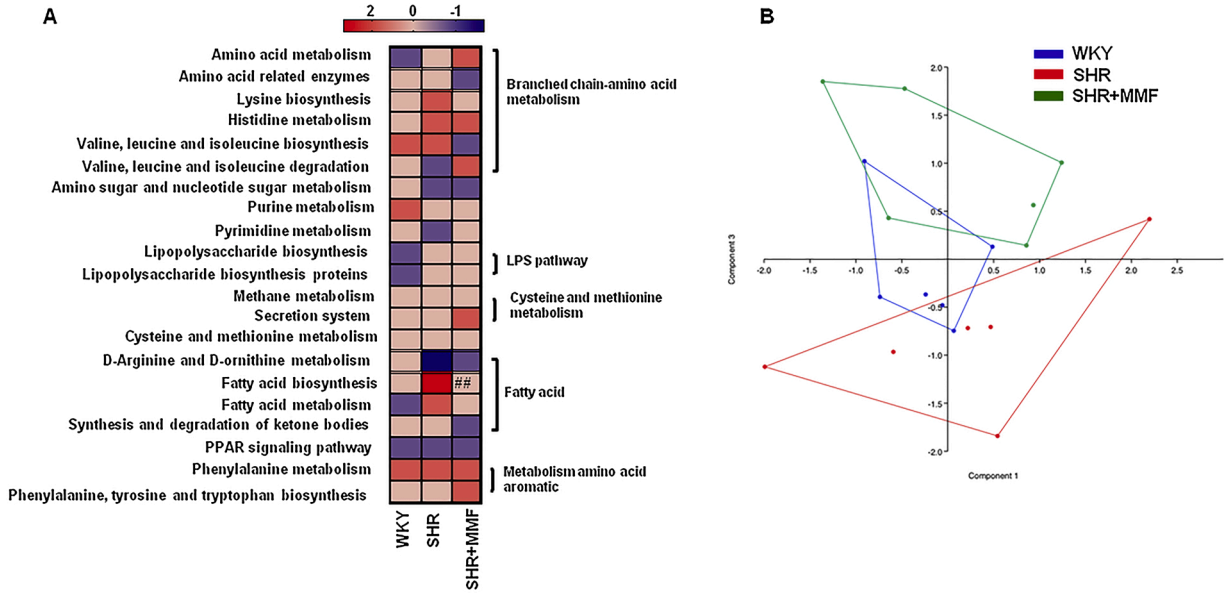

Fig. 5. Mycophenolate mofetil (MMF) induced changes in the gut microbial functions in spontaneously hypertensive rats (SHR). A) The average abundance of KEGG modules differentially enriched in all experimental groups expressed as Z-score. **B)** Principal coordinate analysis in the predictive functional profiling of microbial communities. n = 6 rats per experimental group in each comparison. $^{\#\#}P < 0.01$ significant differences compared with untreated SHR group.

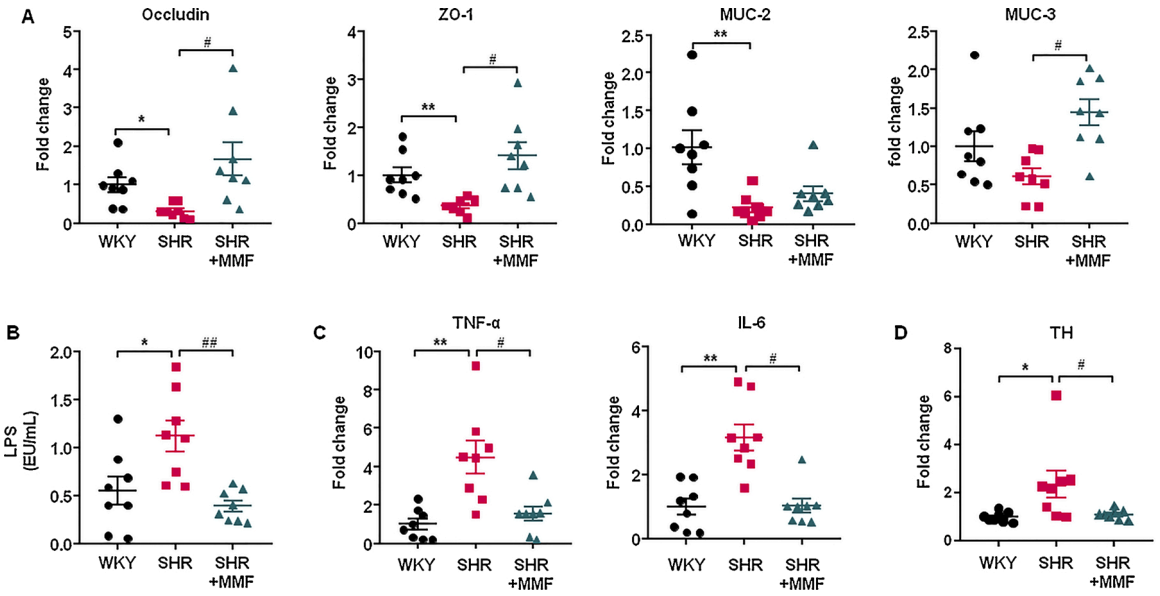

Fig. 6. Mycophenolate mofetil (MMF) induces improvement of gut integrity and inflammation, and gut sympathetic tone in spontaneously hypertensive rats (SHR). A) mRNA levels of occludin, zonula occludens-1 (ZO-1), mucin (MUC)-2, and MUC-3 in colon. B) Levels of plasma endotoxin (endotoxin units/mL (EU/mL). C) Colonic mRNA levels of pro-inflammatory cytokines, tumor necrosis factor-α (TNF-α) and interleukin (IL)-6. D) Colonic tyrosine hydroxylase (TH) expression. Values are expressed as mean ± SEM (n = 7–9). *P < 0.05 and **P < 0.01 compared with WKY group. $^{\#}$P< 0.05 and $^{\#\#}$P< 0.01 significant differences compared to untreated SHR group.

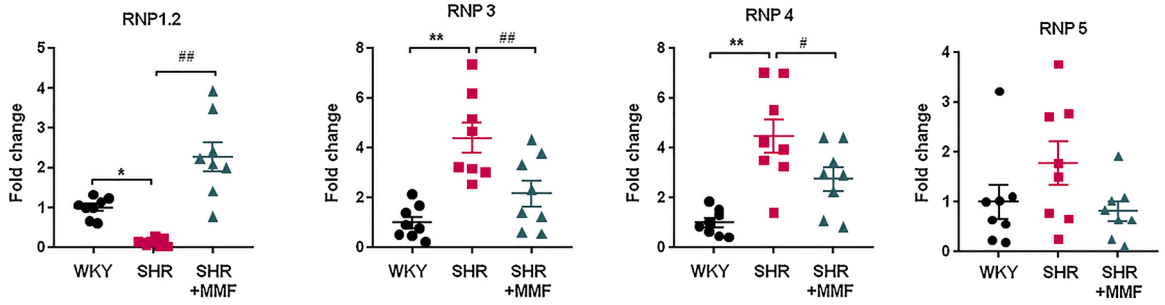

Fig. 7. Mycophenolate mofetil (MMF) induces an improvement in α-defensins production in spontaneously hypertensive rats (SHR). mRNA levels of α-defensins (RNP1.2, RNP3, RNP4, and RNP5) in colon from Wistar Kyoto rats (WKY), untreated SHR (SHR) and SHR treated with MMF (SHR + MMF). Values are expressed as mean ± SEM. *P < 0.05 and **P < 0.01 compared with WKY. $^{\#}$P < 0.05 and $^{\#\#}$P < 0.01 compared with the untreated SHR group.

was elevated in SHR compared to WKY. MMF treatment normalized the content in lymphocytes in MLNs in both hypertensive models (Fig. 8A). The percentage of Treg was reduced in SHR group being it normalized by MMF treatment. The percentage of Th17 lymphocytes was higher in MLNs from SHR compared to WKY group. However, MMF was unable to change Th17 populations in MLNs (Fig. 8B). The level of cytokines produced by Treg (IL10) was found reduced in SHR, being elevated by the MMF treatment. IL17, which is mainly produced by Th17 was found elevated in SHR, and MMF was able to normalize it (Fig. 8C).

3.4. Mycophenolate mofetil (MMF) reduces BP, improves vascular nitric oxide (NO) pathway, and reduced oxidative stress and inflammation in aorta and brain

As was described previously by Tipton et al., [27] in SHR, chronic MMF treatment showed a progressive reduction in SBP (Fig. 9A), which was significative after week 2 of treatment, reaching a total reduction in SHR of 29.5 ± 5.9 mmHg. However, MMF was unable to significant reduce left ventricular hypertrophy in SHR (Fig. 9B). Aortae from hypertensive rats displayed a markedly reduced endothelium-dependent vasodilator responses to acetylcholine compared to control. SHR responses were improved (~ 15 %) after MMF treatment (Fig. 9C). The incubation with L-NAME in the organ bath impeded the normal relaxation induced by acetylcholine in all experimental groups, suggesting NO to be involved in this relaxation (data not shown). Additionally, no differences were found among groups in the endothelium-independent vasodilator responses to the NO donor sodium nitroprusside in aortic rings, discarding changes in the NO pathway in smooth muscle (data not shown). The presence of apocynin in the organ bath increased the relaxation response to acetylcholine in untreated SHR until reaching similar relaxation percentages to those found in control group (data not shown), pointing to the, at least, partial involvement of the increased NADPH oxidase activity in the impaired relaxation to acetylcholine in aorta from SHR. In fact, the NADPH oxidase activity was found reduced in the groups treated with MMF compared to the control groups (Fig. 9D). In addition, aortic segments from SHR displayed a strong increase in ROS contents (Fig. 9E), expressed as red staining to ethidium in vascular wall (~ 27 %). The MMF treatments normalized the vascular ROS in both experimental models (Fig. 9E).

The infiltration of T cells in aorta was analyzed using the mRNA levels of transcription factor FoxP3, retinoid-related orphan receptor-γ (RORγ), and T-bet as markers of accumulation of Treg, Th17, and Th1, respectively (Fig. 10A). Increased Th17 and Th1 cells and reduced Tregs infiltration was shown in aorta from SHR. MMF treatment normalized T

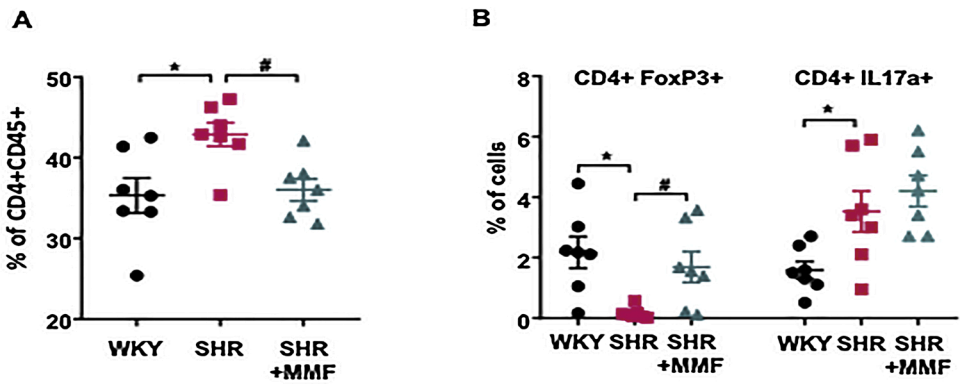

Fig. 8. Mycophenolate (MMF) improves T cell profile at mesenteric lymph nodes (MLNs) in spontaneously hypertensive rats (SHR). A) Total T cells (CD4+CD45+), and, **B)** regulatory T cells (Treg; CD4+ FoxP3+), and T helper (Th)-17 (CD4+ IL17a+) cells in MLNs from all experimental groups. **C)** Concentration of IL-17a and IL-10 was measured by ELISA in lymphocyte conditioned media from MLNs. Values are expressed as mean ± SEM. *P < 0.05 and **P < 0.01 compared with WKY group. #P < 0.05 and ##P < 0.01 significant differences compared with untreated SHR group.

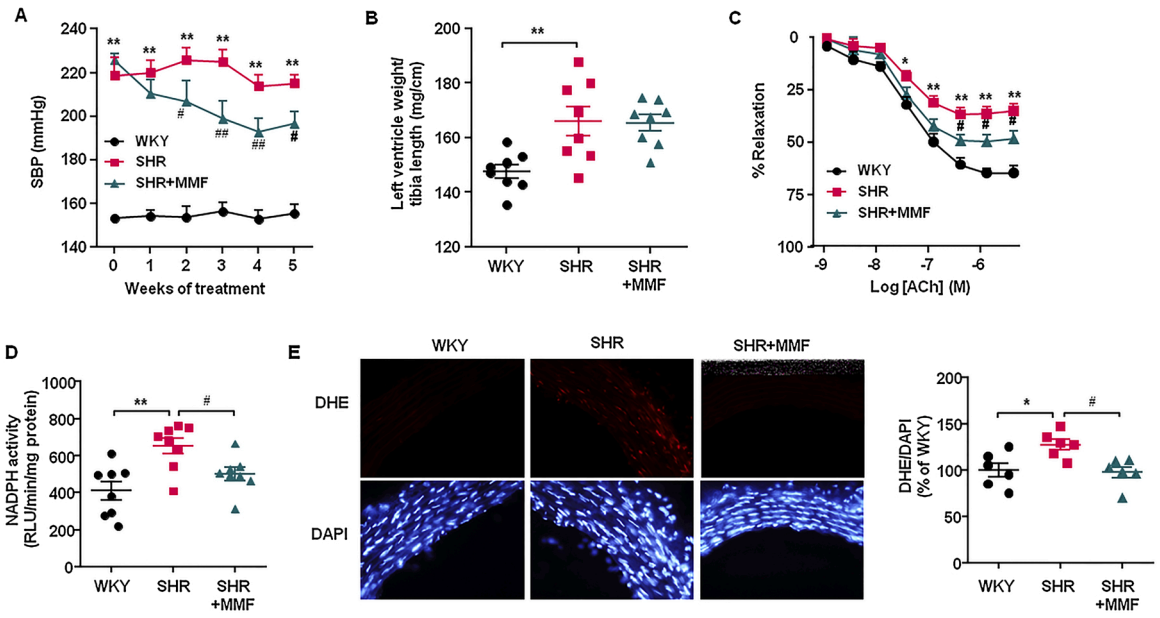

Fig. 9. Mycophenolate mofetil (MMF) reduces blood pressure and endothelial function in aorta from spontaneously hypertensive rats (SHR). A) Time course of systolic blood pressure (SBP) measured by tail-cuff plethysmography. B) Ratio Left ventricle/tibia length (mg/cm). C) Endothelium-dependent relaxation induced by acetylcholine (ACh) in aortas precontracted by phenylephrine. NADPH oxidase activity (D), and *in situ* intracellular ROS (*E*) in aorta from all experimental groups. Values are expressed as mean ± SEM (n = 8). *P < 0.05 and **P < 0.01 significant differences compared with WKY. #P < 0.05 and ##P < 0.01 significant differences compared with untreated SHR group.

cells infiltration in SHR, Interestingly, linked to T cells infiltration, the mRNA levels of the proinflammatory cytokines IL-17a and IFN-γ were higher in SHR (Fig. 10B), as compared to WKY group. Again, the treatment with MMF restored the mRNA levels of these cytokines, whereas increased IL-10 content in aortic homogenates from SHR.

We found that ROS production (Fig. 11A), NADPH oxidase activity (Fig. 11B) and the mRNA levels of CCL2 and CD11b (Fig. 11C) in brain PVN were higher in the SHR group than those found in the WKY group, and were reduced by MMF treatment. In addition, the mRNA levels of pro-inflammatory cytokines (TNF-α, IL-1β, IL-6, and IL-17a) (Fig. 11D) were also increased in SHR and decreased by MMF.

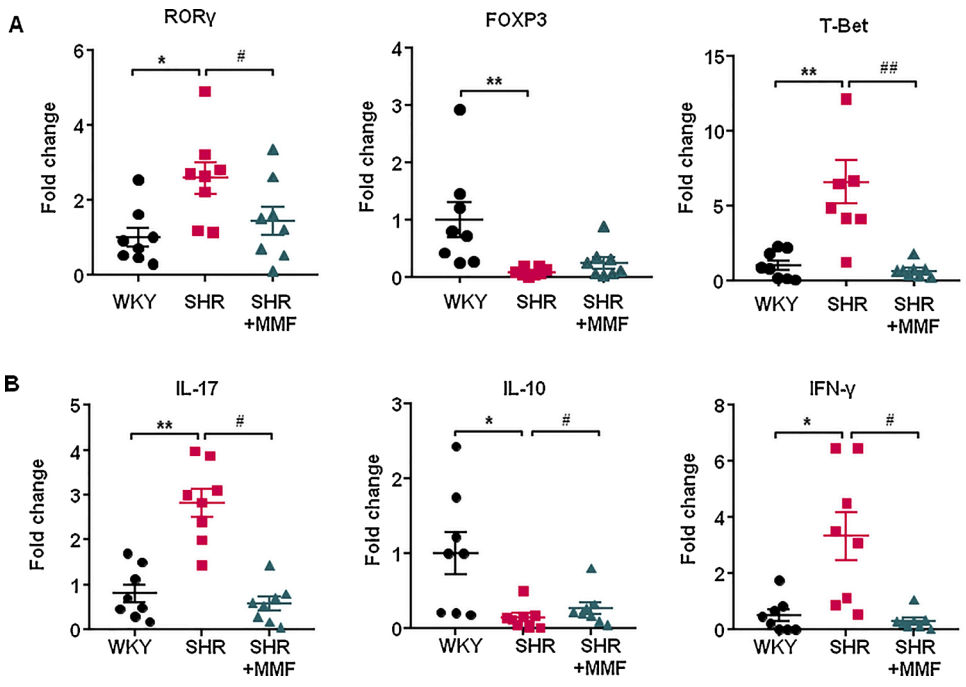

Fig. 10. Mycophenolate mofetil (MMF) induces changes in T cell infiltration in the vascular wall from spontaneously hypertensive rats (SHR). (A) T-cell infiltration in aortas from all experimental groups was measured by mRNA levels of T helper (Th)17; RORγ), regulatory T cells (Treg; FoxP3), and Th1 (T-bet). (B) Cytokine content in aorta from all experimental groups was analyzed by mRNA levels of interleukin (IL) 17a, IL10, and INFγ. Values are expressed as mean ± SEM. *P < 0.05; **P < 0.01 significant differences compared with WKY or CTR. #P < 0.05; ##P < 0.01 significant differences compared with untreated SHR or DOCA.

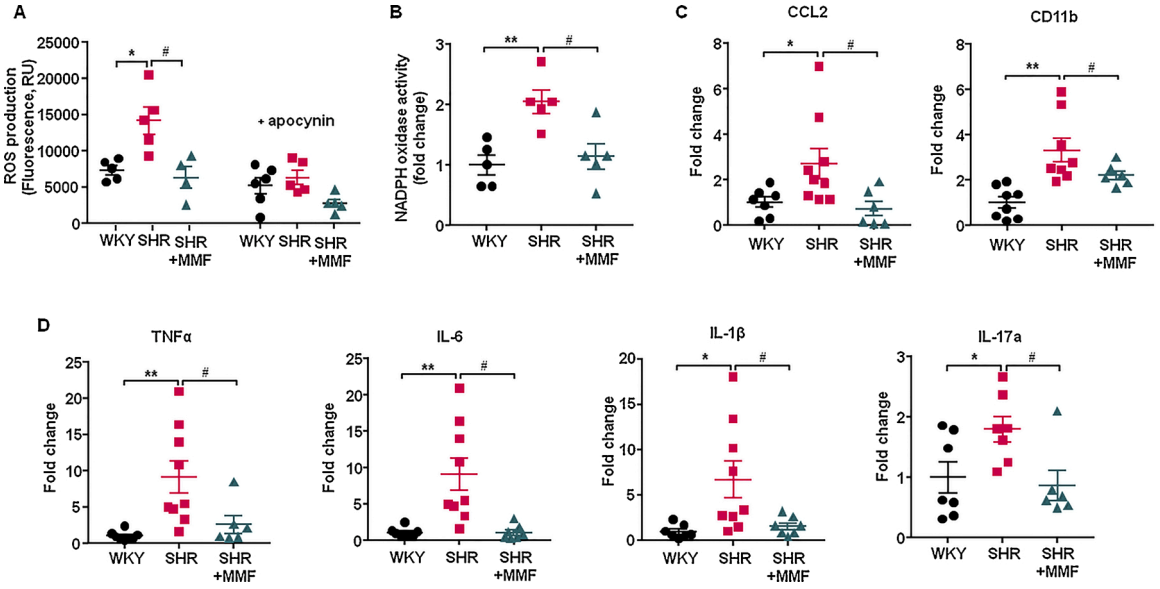

Fig. 11. Mycophenolate mofetil (MMF) reduces immune cells infiltration, neuroinflammation, and NADPH oxidase activity in the paraventricular nucleus (PVN) of the hypothalamus in spontaneously hypertensive rats (SHR) A) CM-H2DCFDA-detected intracellular ROS in absence and presence of NADPH oxidase inhibitor apocynin (50 μM) (n = 4–6). B) NADPH oxidase activity measured by DHE fluorescence measured in the microplate reader in homogenates from brain PVN. (n = 5) C) mRNA levels of C-C Motif Chemokine Ligand 2 (CCL2) and cluster of differentiation molecule 11B (CD11b). D) mRNA levels of pro-inflammatory cytokines, tumor necrosis factor α (TNFα), interleukin (IL)6, IL-1β and IL17a in homogenates from brain PVN of SHR. Values are expressed as mean ± SEM (n = 7–9). *P < 0.05 and **P < 0.01 significant differences compared with WKY. #P < 0.05 and ##P < 0.01 significant differences compared with untreated SHR.

4. Discussion

The principal original findings of this study are as follows: 1) Chronic MMF treatment decreases gut dysbiosis in hypertensive SHR; 2) Shifts in gut microbiota composition induced by MMF were linked to the enhancement of gut integrity and the normalization of colonic α-defensins production, and to the reduction in neuroinflammation and gut sympathetic drive.

Numerous authors have established the link between gut dysbiosis, immune system and hypertension [3,5,6,11,53]. Our results are consistent with what was previously described [18,19,21], being MMF able to induce a reduction in BP in SHR. In addition, MMF improved the endothelial dysfunction joined to a reduction in ROS production as was described by Tian et al. [20]. Furthermore, as already was described [27] MMF treatment induced a modulation in the aortic immune cell infiltration inducing a reduction in the pro-inflammatory cytokines profile.

Several studies have described the ability of immunomodulatory drugs to modulate the gut microbiota inducing dysbiosis [54] or improving the disbiotic condition found in several pathologies [55].

Tacrolimus, a macrolide used for maintenance of immunosuppression in organ transplant recipients, can raise BP, being the elevation induced by tacrolimus dependent on its effect on the intestinal microbiota [28]. Last year it was reported how gut dysbiosis is displayed in diverse experimental models of hypertension [3,5,7–9,55–58] with different characteristics in each model. Our results are in agreement with the key known characteristics of dysbiotic microbiota described in SHR [3,5,7–9,11], such as, a low richness and diversity, a high F/B ratio, and a decrease in acetate- and propionate-producing bacteria, with higher proportions of lactate-producing bacteria. MMF tended to normalize the gut microbiota, regulating the F/B ratio and SCFAs-producing microorganisms.

BP lowering effects of MMF have been associated with decreased circulating and renal T cells in SHR, although MMF reduced both T cell subtypes, Th17 and T-regulatory (Tregs) [27]. However, we found increased Tregs and IL10 (the main cytokine produced from Treg) in both MLNs and aorta from MMF treated rats, which could contribute to their antihypertensive effects, since IL10 released by Tregs improves endothelial function and reduces BP in hypertensive mice [42]. Several authors have described the ability of certain SCFA, as butyrate, to modulate the immune system. Concretely, butyrate is able to induce an elevation in Treg populations [59]. We found an expansion in butyrate-producing bacteria induced by MMF treatment in SHR, which could be involved in the higher numbers of Treg and IL-10 found in MLN and aorta from SHR-MMF group. Surprisily, MMF did not reduce Th17 population in MLNs, taken into account the direct effect of MPA, the active form of MMF, inhibiting IL-17 expression [24]. The lack of inhibitory effect induced by MMF in this gut secondary lymph organ could be related to the elevation in the genus *Sutterella*, which has been described to increase Th17 population [60], found in feces from SHR-MMF group. However, MMF reduced Th17 infiltration in aorta, leading to lower IL17, which could contribute to improve endothelial dysfunction [5]. In addition, the high proportions of *Lactobacillus* ssp. found in SHR were also normalized by the MMF treatment. This is an important beneficial effect because *Lactobacillus* ssp. has been shown to elevate certain pro-inflammatory cytokines as IL-6, TNFα or INFγ [61,62]. Moreover, theses changes in the gut microbiota also entailed modulation in the bacterial synthesis pathways, found a clear different predictive functional profile between WKY *vs* SHR. In particular, in SHR, MMF induced an alteration in the fatty acid pathways.

Multiple possibilities whereby MMF might provoke shifts in gut microbiota were found. It has been repeatedly shown how changes in the host health status are complemented by changes in the composition of gut microbiota. Accordingly, the microbiota could be adapted to BP reduction, shifting to a composition similar to normotensive rats. Nonetheless, we previously demonstrated that hydralazine, which normalized BP in SHR, was unable to improve dysbiosis [8], ruling out the hypothesis that gut microbiota adapted to normotensive conditions. Shifts in the composition of gut microbiota have been linked to gut integrity [4]. The mammalian digestive tract epithelial cells create a tight barrier in the gut, contributing to the hypoxic environment of the lumen. Damage to this barrier makes the environment less hypoxic, conducive to aerobic bacterial growth [63]. In the SHR was found a reduction in the mRNA expression of tight junction proteins, ZO-1 and Occludin, being normalized by the MMF treatment. Increased intestinal permeability in adult hypertensive SHR has been related to reduced goblet cells [49]. These cells produce mucins, which protect the gut from pathogen invasion, were downregulated in hypertensive groups, and treatment with MMF increased its gene expression, suggesting that MMF reduces gut permeability. In fact, MMF inhibited the LPS translocation to the systemic circulation. In addition, intestines of angiotensin II-hypertensive mice and SHR [4,8] were significantly less hypoxic and presented increased aerobic bacteria in feces, due to a reduction in the epithelium barrier integrity. We also found a reduction in the populations of anaerobic bacteria in feces from SHR, which were linked to a loss of gut integrity. MMF-treated SHR displayed an increased colonic integrity and a proportion of strict anaerobic bacteria similar to WKY rats. The data reinforces the essential role of gut integrity in the composition of intestinal microbiota. Furthermore, intestinal epithelial cells and Paneth cells secrete antimicrobial peptides, such as defensins, which selectively kill Gram-positive bacteria [64–67]. Components of bacteria present in the microbiota, such as LPS, are recognized by Toll-like Receptors expressed by these intestinal cells which trigger defensins production and secretion. We found changes in the expression levels of defensins in colonic samples from our hypertensive model compared to WKY group, which might also be involved in changes in microbiota found in SHR. MMF restored defensins expression to become similar to normotensive rats.

These results are consistent with Santisteban et al., [49], evidencing the existence of an increased gut sympathetic drive (higher TH levels) linked to microbial dysbiosis and the lost of gut integrity in hypertensive animals. Robles-Vera et al. [8], demonstrated that reduction of sympathetic activity in the colon induced by losartan improved gut integrity and reduced gut dysbiosis, whereas hydralazine (that increased gut sympathetic drive) was uncapable of restoring gut integrity and microbiota composition. We also found increased mRNA levels of TH in the colon from SHR, which were normalized by MMF treatment. In recent years, the hypothesis that establishes the existence of a brain-gut communication driven by the sympathetic system has gained prevalence. Central administration of a modified tetracycline inhibited microglial activation, normalised sympathetic activity, attenuated pathological alterations in gut wall, restored certain gut microbial communities altered by angiotensin II and reduced BP [68]. Santisteban et al. [49], observed enhanced gut-neuronal communication in hypertension originating from the PVN of the hypothalamus and presenting as increased sympathetic drive to the gut. In brain, angiotensin II *via* an AT1 receptor mechanism activates the sympathetic outflow by stimulation of the NADPH oxidase-dependent ROS production [69]. In brains from SHR, we observed a high NADPH oxidase activity-driven ROS production, and a higher pro-inflammatory cytokine (TNF-α, IL-1β, and IL-6) expression rate than in WKY. The increased sympathetic activity also affects the bone marrow (BM) resulting in an increase in inflammatory cells, which migrate to the PVN and enhance neuroinflammation [48,49]. Accordingly, we found increased inflammation in brain PVN from SHR, linked to increased CCL2 expression levels, which facilitate BM cells entering the brain's parenchymal space; CD11b, a macrophage marker; and IL-17a, mainly produced by Th17 cells, that might contribute to neuroinflammation. MMF reduced immune cells infiltration, neuroinflammation, and NADPH oxidase activity in brain areas of cardiovascular control such as PVN. Our results are in agreement with the reduced brain macrophage/glial activation induced by MMF in stroke-prone SHR [70]. The brain changes induced by MMF in SHR might reduce the sympathetic excitation, lending to lower gut sympathetic drive (lower colonic TH expression). Additionally, the reduced IL-17 levels in the intestine from hypertensive rats treated with MMF can act on sympathetic somata and distal neurites to reducing neurite outgrowth, and improving the neuroanatomical plasticity that accompanies inflammation [71]. The gut sympathetic tone is a crucial modulator of gut barrier integrity and microbiota composition [8,41]. Our results also support this hypothesis because MMF, that reduced colonic TH, improved gut integrity and gut dysbiosis in SHR.

5. Conclusions

We have found for the first time that MMF reduces gut dysbiosis in SHR. This appears to be linked to its ability to improve gut integrity due to reduced sympathetic drive in the gut associated to the decreased brain neuroinflammation.

Declaration of Competing Interest

The authors report no declarations of interest.

Acknowledgments

This work was supported by Grants from Comisión Interministerial de Ciencia y Tecnología, Ministerio de Economía y competitividad (SAF2017-84894-R), Junta de Andalucía (CTS-164) with funds from the European Union, Ministerio de Economia y Competitividad, Instituto de Salud Carlos III (CIBER-CV), Spain. M.T. is a postdoctoral fellow of Instituto de Salud Carlos III (Sara Borrell Program). I.R.-V. is a predoctoral fellow of MINECO. The cost of this publication was paid in part with funds from the European Union (Fondo Europeo de Desarrollo Regional, FEDER, "FEDER una manera de hacer Europa").

References

[1] R.M. Touyz, F.J. Rios, R. Alves-Lopes, K.B. Neves, L.L. Camargo, A.C. Montezano, Oxidative stress: a unifying paradigm in hypertension, Can. J. Cardiol. 36 (5) (2020) 659–670.
[2] T.J. Guzik, N.E. Hoch, K.A. Brown, L.A. McCann, A. Rahman, S. Dikalov, J. Goronzy, C. Weyand, D.G. Harrison, Role of the T cell in the genesis of angiotensin II induced hypertension and vascular dysfunction, J. Exp. Med. 204 (10) (2007) 2449–2460.
[3] T. Yang, M.M. Santisteban, V. Rodriguez, E. Li, N. Ahmari, J.M. Carvajal, M. Zadeh, M. Gong, Y. Qi, J. Zubcevic, B. Sahay, C.J. Pepine, M.K. Raizada, M. Mohamadzadeh, Gut dysbiosis is linked to hypertension, Hypertension 65 (6) (2015) 1331–1340.
[4] S. Kim, R. Goel, A. Kumar, Y. Qi, G. Lobaton, K. Hosaka, M. Mohammed, E. M. Handberg, E.M. Richards, C.J. Pepine, M.K. Raizada, Imbalance of gut microbiome and intestinal epithelial barrier dysfunction in patients with high blood pressure, Clin. Sci. (Lond.) 132 (6) (2018) 701–718.
[5] M. Toral, I. Robles-Vera, N. de la Visitación, M. Romero, M. Sánchez, M. Gómez-Guzmán, A. Rodriguez-Nogales, T. Yang, R. Jiménez, F. Algieri, J. Gálvez, M. K. Raizada, J. Duarte, Role of the immune system in vascular function and blood pressure control induced by faecal microbiota transplantation in rats, Acta Physiol. (Oxf.) 227 (1) (2019), e13285.
[6] S. Sun, A. Lulla, M. Sioda, K. Winglee, M.C. Wu, D.R. Jacobs, J.M. Shikany, D. M. Lloyd-Jones, L.J. Launer, A.A. Fodor, K.A. Meyer, Gut microbiota composition and blood pressure, Hypertension 73 (5) (2019) 998–1006.
[7] T. Yang, V. Aquino, G.O. Lobaton, H. Li, L. Colon-Perez, R. Goel, Y. Qi, J. Zubcevic, M. Febo, E.M. Richards, C.J. Pepine, M.K. Raizada, Sustained captopril-induced reduction in blood pressure is associated with alterations in gut-brain axis in the spontaneously hypertensive rat, J. Am. Heart Assoc. 8 (4) (2019), e010721.
[8] I. Robles-Vera, M. Toral, N. de la Visitación, M. Sánchez, M. Gómez-Guzmán, R. Muñoz, F. Algieri, T. Vezza, R. Jiménez, J. Gálvez, M. Romero, J.M. Redondo, J. Duarte, Changes to the gut microbiota induced by losartan contributes to its antihypertensive effects, Br. J. Pharmacol. 177 (9) (2020) 2006–2023.
[9] I. Robles-Vera, M. Toral, N. de la Visitación, M. Sánchez, M. Gómez-Guzmán, M. Romero, T. Yang, J.L. Izquierdo-Garcia, R. Jiménez, J. Ruiz-Cabello, E. Guerra-Hernández, M.K. Raizada, F. Pérez-Vizcaíno, J. Duarte, Probiotics prevent dysbiosis and the rise in blood pressure in genetic hypertension: role of short-chain fatty acids, Mol. Nutr. Food Res. 64 (6) (2020), e1900616.
[10] J.L. Pluznick, R.J. Protzko, H. Gevorgyan, Z. Peterlin, A. Sipos, J. Han, I. Brunet, L. X. Wan, F. Rey, T. Wang, S.J. Firestein, M. Yanagisawa, J.I. Gordon, A. Eichmann, J. Peti-Peterdi, M.J. Caplan, Olfactory receptor responding to gut microbiota-derived signals plays a role in renin secretion and blood pressure regulation, Proc. Natl. Acad. Sci. U. S. A. 110 (11) (2013) 4410–4415.
[11] J. Li, F. Zhao, Y. Wang, J. Chen, J. Tao, G. Tian, S. Wu, W. Liu, Q. Cui, B. Geng, W. Zhang, R. Weldon, K. Auguste, L. Yang, X. Liu, L. Chen, X. Yang, B. Zhu, J. Cai, Gut microbiota dysbiosis contributes to the development of hypertension, Microbiome 5 (1) (2017) 14.
[12] J.H. Niess, S. Brand, X. Gu, L. Landsman, S. Jung, B.A. McCormick, J.M. Vyas, M. Boes, H.L. Ploegh, J.G. Fox, D.R. Littman, H.C. Reinecker, CX3CR1-mediated dendritic cell access to the intestinal lumen and bacterial clearance, Science 307 (5707) (2005) 254–258.
[13] R.J. Howard, P.R. Patton, A.I. Reed, A.W. Hemming, W.J. Van der Werf, W. W. Pfaff, T.R. Srinivas, J.C. Scornik, The changing causes of graft loss and death after kidney transplantation, Transplantation 73 (12) (2002) 1923–1928.
[14] P.L. Huang, Z. Huang, H. Mashimo, K.D. Bloch, M.A. Moskowitz, J.A. Bevan, M. C. Fishman, Hypertension in mice lacking the gene for endothelial nitric oxide synthase, Nature 377 (6546) (1995) 239–242.
[15] V.L. Chiasson, D. Talreja, K.J. Young, P. Chatterjee, A.K. Banes-Berceli, B. M. Mitchell, FK506 binding protein 12 deficiency in endothelial and hematopoietic cells decreases regulatory T cells and causes hypertension, Hypertension 57 (6) (2011) 1167–1175.
[16] B. Rodríguez-Iturbe, H. Pons, Y. Quiroz, K. Gordon, J. Rincón, M. Chávez, G. Parra, J. Herrera-Acosta, D. Gómez-Garre, R. Largo, J. Egido, R.J. Johnson, Mycophenolate mofetil prevents salt-sensitive hypertension resulting from angiotensin II exposure, Kidney Int. 59 (6) (2001) 2222–2232.
[17] Y. Quiroz, H. Pons, K.L. Gordon, J. Rincón, M. Chávez, G. Parra, J. Herrera-Acosta, D. Gómez-Garre, R. Largo, J. Egido, R.J. Johnson, B. Rodríguez-Iturbe, Mycophenolate mofetil prevents salt-sensitive hypertension resulting from nitric oxide synthesis inhibition, Am. J. Physiol. Renal Physiol. 281 (1) (2001) F38–47.
[18] B. Rodríguez-Iturbe, Y. Quiroz, M. Nava, L. Bonet, M. Chávez, J. Herrera-Acosta, R. J. Johnson, H.A. Pons, Reduction of renal immune cell infiltration results in blood pressure control in genetically hypertensive rats, Am. J. Physiol. Renal Physiol. 282 (2) (2002) F191–201.
[19] D.L. Mattson, L. James, E.A. Berdan, C.J. Meister, Immune suppression attenuates hypertension and renal disease in the Dahl salt-sensitive rat, Hypertension 48 (1) (2006) 149–156.
[20] N. Tian, J.W. Gu, S. Jordan, R.A. Rose, M.D. Hughson, R.D. Manning, Immune suppression prevents renal damage and dysfunction and reduces arterial pressure in salt-sensitive hypertension, Am. J. Physiol. Heart Circ. Physiol. 292 (2) (2007) H1018–25.
[21] A.D. Moes, D. Severs, K. Verdonk, N. van der Lubbe, R. Zietse, A.H.J. Danser, E. J. Hoorn, Mycophenolate mofetil attenuates DOCA-salt hypertension: effects on vascular tone, Front. Physiol. 9 (2018) 578.
[22] Y. Takeda, I. Miyamori, K. Furukawa, S. Inaba, H. Mabuchi, Mechanisms of FK 506-induced hypertension in the rat, Hypertension 33 (1) (1999) 130–136.
[23] M.C. Braun, S.M. Herring, N. Gokul, M. Monita, R. Bell, Y. Zhu, M.L. Gonzalez-Garay, S.E. Wenderfer, P.A. Doris, Hypertensive renal injury is associated with gene variation affecting immune signaling, Circ. Cardiovasc. Genet. 7 (6) (2014) 903–910.
[24] F. Abadja, C. Videcoq, E. Alamartine, F. Berthoux, C. Mariat, Differential effect of cyclosporine and mycophenolic acid on the human regulatory T cells and TH-17 cells balance, Transplant. Proc. 41 (8) (2009) 3367–3370.
[25] S. Slight-Webb, J.M. Guthridge, E.F. Chakravarty, H. Chen, R. Lu, S. Macwana, K. Bean, H.T. Maecker, P.J. Utz, J.A. James, Mycophenolate mofetil reduces STAT3 phosphorylation in systemic lupus erythematosus patients, JCI Insight 4 (2) (2019).
[26] F. Abadja, S. Atemkeng, E. Alamartine, F. Berthoux, C. Mariat, Impact of mycophenolic acid and tacrolimus on Th17-related immune response, Transplantation 92 (4) (2011) 396–403.
[27] A.J. Tipton, B. Baban, J.C. Sullivan, Female spontaneously hypertensive rats have greater renal anti-inflammatory T lymphocyte infiltration than males, Am. J. Physiol. Regul. Integr. Comp. Physiol. 303 (4) (2012) R359–67.
[28] M. Toral, M. Romero, A. Rodríguez-Nogales, R. Jiménez, I. Robles-Vera, F. Algieri, N. Chueca-Porcuna, M. Sánchez, N. de la Visitación, M. Olivares, F. García, F. Pérez-Vizcaíno, J. Gálvez, J. Duarte, Lactobacillus fermentum improves tacrolimus-induced hypertension by restoring vascular redox state and improving eNOS coupling, Mol. Nutr. Food Res. (2018), e1800033.
[29] K.L. Flannigan, T. Rajbar, A. Moffat, L.S. McKenzie, F. Dicke, K. Rioux, M. L. Workentine, T.J. Louie, S.A. Hirota, S.C. Greenway, Changes in composition of the gut bacterial microbiome after fecal microbiota transplantation for recurrent, Front. Cardiovasc. Med. 4 (2017) 17.
[30] G. Zaza, A. Dalla Gassa, G. Felis, S. Granata, S. Torriani, A. Lupo, Impact of maintenance immunosuppressive therapy on the fecal microbiome of renal transplant recipients: comparison between an everolimus- and a standard tacrolimus-based regimen, PLoS One 12 (5) (2017), e0178228.
[31] J.C. Swarte, R.M. Douwes, S. Hu, A. Vich Vila, M.F. Eisenga, M. van Londen, A. W. Gomes-Neto, R.K. Weersma, H.J.M. Harmsen, S.J.L. Bakker, Characteristics and dysbiosis of the gut microbiome in renal transplant recipients, J. Clin. Med. 9 (2) (2020).
[32] C.M. Gibson, L.M. Childs-Kean, Z. Naziruddin, C.K. Howell, The alteration of the gut microbiome by immunosuppressive agents used in solid organ transplantation, Transpl. Infect. Dis. (2020), e13397.
[33] J. Tourret, N. Benabdellah, S. Drouin, F. Charlotte, J. Rottembourg, N. Arzouk, A. Fekkar, B. Barrou, Unique case report of a chromomycosis and Listeria in soft tissue and cerebellar abscesses after kidney transplantation, BMC Infect. Dis. 17 (1) (2017) 288.
[34] K.L. Flannigan, M.R. Taylor, S.K. Pereira, J. Rodriguez-Arguello, A.W. Moffat, L. Alston, X. Wang, K.K. Poon, P.L. Beck, K.P. Rioux, M. Jonnalagadda, P. K. Chelikani, H.J. Galipeau, I.A. Lewis, M.L. Workentine, S.C. Greenway, S. A. Hirota, An intact microbiota is required for the gastrointestinal toxicity of the immunosuppressant mycophenolate mofetil, J. Heart Lung Transplant. 37 (9) (2018) 1047–1059.
[35] M.R. Taylor, K.L. Flannigan, H. Rahim, A. Mohamud, I.A. Lewis, S.A. Hirota, S. C. Greenway, Vancomycin relieves mycophenolate mofetil-induced gastrointestinal toxicity by eliminating gut bacterial β-glucuronidase activity, Sci. Adv. 5 (8) (2019) eaax2358.
[36] J. Tourret, B.P. Willing, S. Dion, J. MacPherson, E. Denamur, B.B. Finlay, Immunosuppressive treatment alters secretion of ileal antimicrobial peptides and gut microbiota, and favors subsequent colonization by uropathogenic Escherichia coli, Transplantation 101 (1) (2017) 74–82.
[37] J.C. McGrath, E. Lilley, Implementing guidelines on reporting research using animals (ARRIVE etc.): new requirements for publication in BJP, Br. J. Pharmacol. 172 (13) (2015) 3189–3193.
[38] R. Vera, R. Jiménez, F. Lodi, M. Sánchez, M. Galisteo, A. Zarzuelo, F. Pérez-Vizcaíno, J. Duarte, Genistein restores caveolin-1 and AT-1 receptor expression and vascular function in large vessels of ovariectomized hypertensive rats, Menopause 14 (5) (2007) 933–940.
[39] M. Gómez-Guzmán, R. Jiménez, M. Sánchez, M. Romero, F. O'Valle, R. Lopez-Sepulveda, A.M. Quintela, P. Galindo, M.J. Zarzuelo, E. Bailón, E. Delpón, F. Perez-Vizcaino, J. Duarte, Chronic (-)-epicatechin improves vascular oxidative and inflammatory status but not hypertension in chronic nitric oxide-deficient rats, Br. J. Nutr. 106 (9) (2011) 1337–1348.
[40] M.J. Zarzuelo, R. Jiménez, P. Galindo, M. Sánchez, A. Nieto, M. Romero, A. M. Quintela, R. López-Sepúlveda, M. Gómez-Guzmán, E. Bailón, I. Rodríguez-Gómez, A. Zarzuelo, J. Gálvez, J. Tamargo, F. Pérez-Vizcaíno, J. Duarte,

Antihypertensive effects of peroxisome proliferator-activated receptor-β activation in spontaneously hypertensive rats, Hypertension 58 (4) (2011) 733–743.
[41] M. Toral, I. Robles-Vera, N. de la Visitación, M. Romero, T. Yang, M. Sánchez, M. Gómez-Guzmán, R. Jiménez, M.K. Raizada, J. Duarte, Critical role of the interaction gut microbiota-sympathetic nervous system in the regulation of blood pressure, Front. Physiol. 10 (2019) 231.
[42] M. Kassan, M. Galan, M. Partyka, M. Trebak, K. Matrougui, Interleukin-10 released by CD4(+)CD25(+) natural regulatory T cells improves microvascular endothelial function through inhibition of NADPH oxidase activity in hypertensive mice, Arterioscler. Thromb. Vasc. Biol. 31 (11) (2011) 2534–2542.
[43] M. Romero, M. Toral, I. Robles-Vera, M. Sánchez, R. Jiménez, F. O'Valle, A. Rodriguez-Nogales, F. Pérez-Vizcaino, J. Gálvez, J. Duarte, Activation of peroxisome proliferator activator receptor β/δ improves endothelial dysfunction and protects kidney in murine lupus, Hypertension 69 (4) (2017) 641–650.
[44] N. Segata, J. Izard, L. Waldron, D. Gevers, L. Miropolsky, W.S. Garrett, C. Huttenhower, Metagenomic biomarker discovery and explanation, Genome Biol. 12 (6) (2011) R60.
[45] B. Sánchez, I. González-Rodríguez, S. Arboleya, P. López, A. Suárez, P. Ruas-Madiedo, A. Margolles, M. Gueimonde, The effects of Bifidobacterium breve on immune mediators and proteome of HT29 cells monolayers, Biomed Res. Int. 2015 (2015), 479140.
[46] Y.H. Ding, L.Y. Qian, J. Pang, J.Y. Lin, Q. Xu, L.H. Wang, D.S. Huang, H. Zou, The regulation of immune cells by Lactobacilli: a potential therapeutic target for anti-atherosclerosis therapy, Oncotarget 8 (35) (2017) 59915–59928.
[47] N.O. Kaakoush, Sutterella species, IgA-degrading bacteria in ulcerative colitis, Trends Microbiol. 28 (7) (2020) 519–522.
[48] M.M. Santisteban, N. Ahmari, J.M. Carvajal, M.B. Zingler, Y. Qi, S. Kim, J. Joseph, F. Garcia-Pereira, R.D. Johnson, V. Shenoy, M.K. Raizada, J. Zubcevic, Involvement of bone marrow cells and neuroinflammation in hypertension, Circ. Res. 117 (2) (2015) 178–191.
[49] M.M. Santisteban, Y. Qi, J. Zubcevic, S. Kim, T. Yang, V. Shenoy, C.T. Cole-Jeffrey, G.O. Lobaton, D.C. Stewart, A. Rubiano, C.S. Simmons, F. Garcia-Pereira, R. D. Johnson, C.J. Pepine, M.K. Raizada, Hypertension-linked pathophysiological alterations in the gut, Circ. Res. 120 (2) (2017) 312–323.
[50] A.M. Mowat, W.W. Agace, Regional specialization within the intestinal immune system, Nat. Rev. Immunol. 14 (10) (2014) 667–685.
[51] C.L. Bevins, Events at the host-microbial interface of the gastrointestinal tract. V. Paneth cell alpha-defensins in intestinal host defense, Am. J. Physiol. Gastrointest. Liver Physiol. 289 (2) (2005) G173–6.
[52] T. Hashimoto, T. Perlot, A. Rehman, J. Trichereau, H. Ishiguro, M. Paolino, V. Sigl, T. Hanada, R. Hanada, S. Lipinski, B. Wild, S.M. Camargo, D. Singer, A. Richter, K. Kuba, A. Fukamizu, S. Schreiber, H. Clevers, F. Verrey, P. Rosenstiel, J. M. Penninger, ACE2 links amino acid malnutrition to microbial ecology and intestinal inflammation, Nature 487 (7408) (2012) 477–481.
[53] B. Mell, V.R. Jala, A.V. Mathew, J. Byun, H. Waghulde, Y. Zhang, B. Haribabu, M. Vijay-Kumar, S. Pennathur, B. Joe, Evidence for a link between gut microbiota and hypertension in the Dahl rat, Physiol. Genom. 47 (6) (2015) 187–197.
[54] R. Bodkhe, B. Balakrishnan, V. Taneja, The role of microbiome in rheumatoid arthritis treatment, Ther. Adv. Musculoskelet. Dis. 11 (2019), 1759720X19844632.
[55] M. Qiu, K. Huang, Y. Liu, Y. Yang, H. Tang, X. Liu, C. Wang, H. Chen, Y. Xiong, J. Zhang, J. Yang, Modulation of intestinal microbiota by glycyrrhizic acid prevents high-fat diet-enhanced pre-metastatic niche formation and metastasis, Mucosal Immunol. 12 (4) (2019) 945–957.
[56] F.Z. Marques, E. Nelson, P.Y. Chu, D. Horlock, A. Fiedler, M. Ziemann, J.K. Tan, S. Kuruppu, N.W. Rajapakse, A. El-Osta, C.R. Mackay, D.M. Kaye, High-fiber diet and acetate supplementation change the gut microbiota and prevent the development of hypertension and heart failure in hypertensive mice, Circulation 135 (10) (2017) 964–977.
[57] I. Robles-Vera, M. Toral, N. de la Visitación, M. Sánchez, M. Romero, M. Olivares, R. Jiménez, J. Duarte, The probiotic Lactobacillus fermentum prevents dysbiosis and vascular oxidative stress in rats with hypertension induced by chronic nitric oxide blockade, Mol. Nutr. Food Res. 62 (19) (2018), e1800298.
[58] I. Robles-Vera, N. de la Visitación, M. Toral, M. Sánchez, M. Romero, M. Gómez-Guzmán, T. Yang, J.L. Izquierdo-García, E. Guerra-Hernández, J. Ruiz-Cabello, M. K. Raizada, F. Pérez-Vizcaíno, R. Jiménez, J. Duarte, Probiotic Bifidobacterium breve prevents DOCA-salt hypertension, FASEB J. 34 (10) (2020) 13626–13640.
[59] A.M. Tyagi, M. Yu, T.M. Darby, C. Vaccaro, J.Y. Li, J.A. Owens, E. Hsu, J. Adams, M.N. Weitzmann, R.M. Jones, R. Pacifici, The microbial metabolite butyrate stimulates bone formation via T regulatory cell-mediated regulation of WNT10B expression, Immunity 49 (6) (2018) 1116–1131, e7.
[60] K. Hiippala, V. Kainulainen, M. Kalliomäki, P. Arkkila, R. Satokari, Mucosal prevalence and interactions with the epithelium indicate commensalism of, Front. Microbiol. 7 (2016) 1706.
[61] N. Reilly, V. Poylin, M. Menconi, A. Onderdonk, S. Bengmark, P.O. Hasselgren, Probiotics potentiate IL-6 production in IL-1beta-treated Caco-2 cells through a heat shock-dependent mechanism, Am. J. Physiol. Regul. Integr. Comp. Physiol. 293 (3) (2007) R1169–79.
[62] L.M. Rocha-Ramírez, R.A. Pérez-Solano, S.L. Castañón-Alonso, S.S. Moreno Guerrero, A. Ramírez Pacheco, M. García Garibay, C. Eslava, Probiotic, J. Immunol. Res. (2017), 4607491.
[63] Z.M. Earley, S. Akhtar, S.J. Green, A. Naqib, O. Khan, A.R. Cannon, A.M. Hammer, N.L. Morris, X. Li, J.M. Eberhardt, R.L. Gamelli, R.H. Kennedy, M.A. Choudhry, Burn injury alters the intestinal microbiome and increases gut permeability and bacterial translocation, PLoS One 10 (7) (2015), e0129996.
[64] T. Ayabe, D.P. Satchell, C.L. Wilson, W.C. Parks, M.E. Selsted, A.J. Ouellette, Secretion of microbicidal alpha-defensins by intestinal Paneth cells in response to bacteria, Nat. Immunol. 1 (2) (2000) 113–118.
[65] P. Vora, A. Youdim, L.S. Thomas, M. Fukata, S.Y. Tesfay, K. Lukasek, K. S. Michelsen, A. Wada, T. Hirayama, M. Arditi, M.T. Abreu, Beta-defensin-2 expression is regulated by TLR signaling in intestinal epithelial cells, J. Immunol. 173 (9) (2004) 5398–5405.
[66] E.G. Pamer, Immune responses to commensal and environmental microbes, Nat. Immunol. 8 (11) (2007) 1173–1178.
[67] S. Vaishnava, C.L. Behrendt, A.S. Ismail, L. Eckmann, L.V. Hooper, Paneth cells directly sense gut commensals and maintain homeostasis at the intestinal host-microbial interface, Proc. Natl. Acad. Sci. U. S. A. 105 (52) (2008) 20858–20863.
[68] R.K. Sharma, T. Yang, A.C. Oliveira, G.O. Lobaton, V. Aquino, K. Kim, E. M. Richards, C.J. Pepine, C. Sumners, M.K. Raizada, Microglial cells impact gut microbiota and gut pathology in angiotensin II-Induced hypertension, Circ. Res. 124 (5) (2019) 727–736.
[69] L. Gao, W. Wang, Y.L. Li, H.D. Schultz, D. Liu, K.G. Cornish, I.H. Zucker, Sympathoexcitation by central ANG II: roles for AT1 receptor upregulation and NAD(P)H oxidase in RVLM, Am. J. Physiol. Heart Circ. Physiol. 288 (5) (2005) H2271–9.
[70] I.S. Dhande, Y. Zhu, M.C. Braun, M.J. Hicks, S.E. Wenderfer, P.A. Doris, Mycophenolate mofetil prevents cerebrovascular injury in stroke-prone spontaneously hypertensive rats, Physiol. Genom. 49 (3) (2017) 132–140.
[71] S.P. Chisholm, A.L. Cervi, S. Nagpal, A.E. Lomax, Interleukin-17A increases neurite outgrowth from adult postganglionic sympathetic neurons, J. Neurosci. 32 (4) (2012) 1146–1155.